

HCN from the Reduction of NO over Platinum, Palladium, Ruthenium, Monel and Perovskite Catalysts

R. J. H. VOORHOEVE, C. K. N. PATEL, L. E. TRIMBLE,
R. J. KERL, AND P. K. GALLAGHER

Bell Laboratories, Murray Hill, New Jersey 07974

Received April 29, 1976; revised August 30, 1976

HCN was produced in mixtures of NO, CO and H₂ at temperatures from 400–800°C. Most active in HCN production was a supported Pt catalyst, followed by Pd, Cu–Ni and Ru, in that order. Perovskite La_{0.8}K_{0.2}MnO₃ yields little HCN, but over La_{0.8}K_{0.2}Mn_{0.94}Ru_{0.06}O₃ the yield is higher than over either Ru or the matrix perovskite. The effects of water vapor concentration and space velocity on the yield of HCN were studied. The formation of HCN is tentatively explained on the basis of an intermediate of composition [NCO], which may be an isocyanate.

INTRODUCTION

The thermodynamic stability of HCN makes its formation possible, at least in principle, from any gas mixtures containing N, C and H (1, 2). Commercially, HCN is produced by reacting CH₄ and NH₃ at approximately 1000°C over Pt, Pt–Rh or Pt–Ru wire gauze catalysts (3). In the course of our study of the reduction of NO with CO and H₂ in concentrations similar to those in auto exhaust, the formation of HCN over Pt catalysts was recently discovered at medium temperatures of 500–800°C (4). Subsequent dynamometer tests of the Gould Inc. dual bed catalyst system (a train of a Pt oxygen scavenger catalyst, a monel reduction catalyst and a Pt oxidation catalyst) showed only insignificant HCN levels down stream from the oxidation catalyst, but did not check the consequences of a failure of either the airpump or the oxidation catalyst (5). In contrast, automotive tests with three-way catalysts containing Pt/Pd and Pt/Rh as the active components showed quite significant HCN

levels when rich carburetion prevailed due to failure of the oxygen sensor in the control loop. Levels as high as 60–90 ppm HCN were measured even in the presence of 0.03 wt% S in the fuel (6). Apparently, under automotive conditions, HCN formation is not as effectively reduced by SO₂ and H₂O as suggested by laboratory tests (4, 5).

The present paper is an extension of our earlier study and includes exploratory investigations of the formation of HCN from CO, H₂ and NO over metallic Ru, Pd and Pt, over a Cu–Ni (Monel) alloy and over two perovskite catalysts, viz, La_{0.8}K_{0.2}MnO₃ and La_{0.8}K_{0.2}Mn_{0.94}Ru_{0.06}O₃. The details of the reduction of NO to N₂ and NH₃ over several of these catalysts have been published recently (7–10), but the formation of HCN was not studied in those papers. The present paper concentrates on the yield of HCN obtained over the various catalysts under a set of standard conditions. The catalysts were studied in a conventional flow reactor, with HCN in the effluent analyzed by a newly developed

TABLE 1
Relative Sensitivities for the Detection
of HCN, NH₃ and H₂O^a

CO laser		OA signal		
Line	Fre- quency cm ⁻¹	HCN (1000 ppm)	H ₂ O (10,000 ppm)	NH ₃ (1000 ppm)
<i>P</i> ₂₇₋₂₆ (12)	1442.15	50.0	<10 ⁻³	<10 ⁻³
<i>P</i> ₂₆₋₂₅ (15)	1456.02	<10 ⁻⁵	4.8	<10 ⁻²
<i>P</i> ₂₀₋₁₉ (14)	1605.27	<10 ⁻⁴	<10 ⁻³	8.0

^a Normalized to power level on each of the laser lines; at a total gas pressure of 60 Torr in the OA cell.

infrared absorption technique employing opto-acoustic (OA) detection, which is a technique similar to that used previously by some of us to analyze for NO in the troposphere and for atmospheric pollutants (11-13). On some of the catalysts, thermal desorption analysis was performed with mass-spectrometric detection of the desorbed products, after equilibration of the catalysts in the catalytic process.

EXPERIMENTAL METHODS

The catalytic test equipment consisted of a vertical quartz tubular reactor with a fixed bed made up from an appropriate

amount of catalyst (1-2 g) mixed with low surface area inert α -Al₂O₃ chips to bring the bed volume to 1 cm³. A sheathed thermocouple was placed in the center of the bed. The catalyst was subjected to a downward flow of the gas mixture, which consisted of NO (0.1-0.3%), H₂ (0.2-0.5%), CO (3-5%) and H₂O (0-4%) diluted with He. The gases were mixed in-line and the inlet composition before the reactor was monitored continuously by gas chromatography. The product mixture was automatically sampled and analyzed by two on-line gas chromatographs (gc). One gc, fitted with a Porapak Q and a molecular sieve 13x column, separated NO, CO, N₂O, N₂, O₂, H₂ and CO₂ (5). The other gc, fitted with a Porapak R column and/or a Porapak Q column, separated CO₂, N₂O, NH₃, H₂O and HCN.

Part of the reactor effluent continuously passed through a pressure-reducing valve and subsequently through the opto-acoustic cell for infrared analysis of HCN, NH₃ and H₂O. HCN yields reported in this paper are those determined by the ir technique.

The CO laser based technique briefly described in Ref. (4) for HCN and H₂O measurements was expanded to include determination of NH₃ by proper choice of a fourth laser wavelength as seen from

TABLE 2
Description of Catalysts Used

Name	Composition	Preparation	Surface area (m ² /g)	Ref. ^a
Ru	Ru, 99.999%	United Mineral and Chemical Corp.	0.35	(7)
Pd	Pd, 99.999%	United Mineral and Chemical Corp.	0.40	
Pt I	0.2% Pt on cordierite	Engelhard PTX-3 crushed	0.07 ^b	
Pt II	Pt, 99.99%	Engelhard sponge	0.12	
Cu-Ni	Cu:Ni = 0.64:1(at/at) ^c	Filings of commercial monel alloy	0.12	
PER	La _{0.9} K _{0.2} MnO ₃	J. P. Remeika	2.50	(8)
PER-Ru	La _{0.8} K _{0.2} Mn _{0.94} Ru _{0.06} O ₃	J. P. Remeika	1.00	(10)

^a Reference to studies of the selectivity and activity of the reduction of NO to N₂, N₂O and NH₃ over the same catalysts and to preparation of perovskite catalysts.

^b Pt area only, as determined by H₂ chemisorption.

^c Cu + Ni is 97%. Analysis by Fairfield Testing Labs, Fairfield, N.J.

Table 1. In addition, refinements were introduced in the grating drive for controlling the CO laser oscillation frequency to obtain greater reproducibility. In our earlier paper (4), measurements of HCN concentrations below 5 ppm were limited by our ability to reset the grating to the desired position (after having scanned the wavelengths listed in Table 1) so that a cavity resonance fell exactly at the center of the gain curve corresponding to a CO laser transition. Inability to do so results not only in the output power on a given CO laser line changing every time we come back to the line but also in the output frequency from the laser being variable to $\sim \pm \Delta\nu_{D/2}$ from that given in Table 1 where $\Delta\nu_D$ is

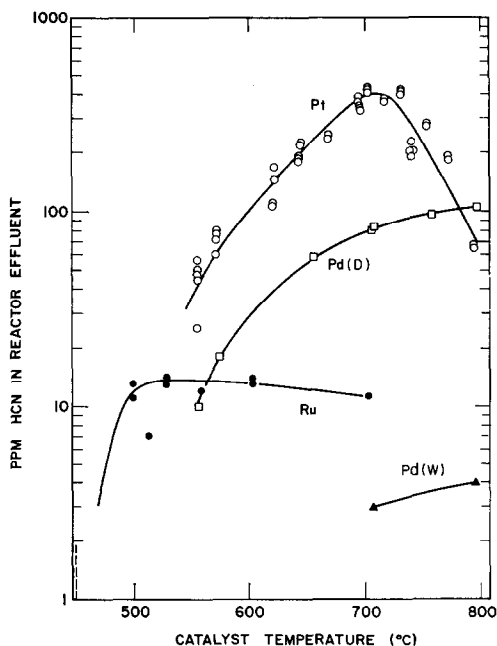


FIG. 1. Yield of HCN as a function of catalyst temperature for unsupported Ru, Pd and Pt II catalysts. Flow rates are 2.3×10^4 ml hr^{-1} m^{-2} for Pt II, 1.22×10^5 ml hr^{-1} m^{-2} for Pd and 3.14×10^5 ml hr^{-1} m^{-2} for Ru. The broken vertical line at 455°C indicates the highest temperature at which no HCN was found for the Ru catalyst. Pd(W) is for the standard mixture with 3.5% H_2O added, the other curves are for the standard mixture (5% CO, 0.5% H_2 , 0.3% NO, balance He).

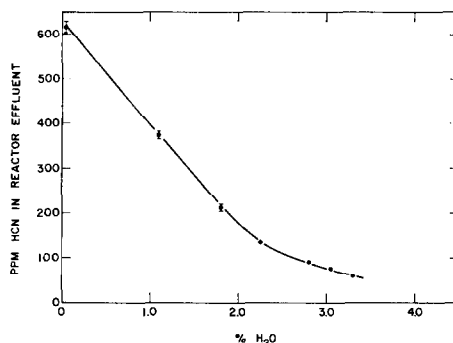


FIG. 2. Effect of the partial pressure of water on the yield of HCN in a mixture of 5% CO, 0.5% H_2 , 0.3% NO and $x\%$ H_2O in He at a flow rate of 3.8×10^5 ml hr^{-1} m^{-2} . Temperature 709°C. Catalyst Pt-I (PTX).

the Doppler width of CO lasing molecule. Since $\Delta\nu_D = 150$ MHz, the lack of resetability to ± 75 MHz was seen to cause irreproducible results. This was cured by inclusion of a servo control of the cavity length so that laser oscillation frequency remained essentially at the center of the corresponding CO laser transition. Improvement of about a factor of 5 was obtained over that reported in Ref. (4). The smallest HCN concentration that can be reliably measured is now estimated to be 1 ppm.

Evolved gas analysis (EGA) was performed by heating about 0.1 g of sample in an evacuated SiO_2 tube. The surrounding furnace was programmed to heat at a rate of about 2°C min^{-1} . The tube was evacuated by a turbomolecular pump. An AEI, MS-10 mass spectrometer was inserted between the sample and the pump. The mass range from 12-45 was constantly cycled and the output of the mass spectrometer was fed to an Infotronics Model CS-204 integrator. The timing was reset for each cycle (~ 13 min) by a microswitch closure on the mass spectrometer. The background pressure in the absence of decomposition is about 2×10^{-7} Torr.

The catalysts used are described in Table 2. The gases used were obtained diluted in He from Scientific Gas Products, Inc. The

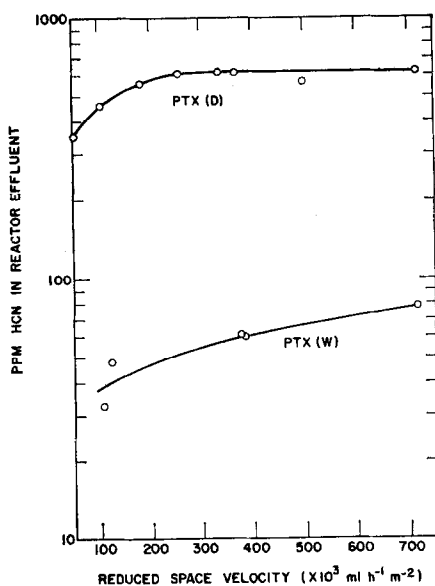


FIG. 3. Variation of the yield of HCN at 709°C with flow rate for the Pt-I (PTX) catalyst in the standard mixture and in the standard mixture with 3.5% H₂O.

surface areas were determined with a Micromeritics Model 2100D Orr surface area analyzer or with a Perkin-Elmer Sorptionmeter.

RESULTS AND DISCUSSION

Platinum

The results published previously (4) for the Pt I and Pt II catalysts showed that both catalysts behaved in a quite similar way. In a mixture of 5% CO, 0.5% H₂ and 0.3% NO in He (the "standard" mixture), the HCN yield became measurable at about 500°C, reached a broad maximum at approximately 700°C and then declined somewhat faster for the sponge Pt II catalyst than for the supported Pt I. The data for the sponge Pt-II are reproduced in Fig. 1 for comparison with the other noble metals. The effect of 3.5% H₂O in the inlet was to decrease the HCN yield by an order of magnitude over the range 550–800°C. Figure 2 shows the effect of water in the standard mixture on the

yield of HCN at 709°C for the Pt-I catalyst. The yield of HCN is somewhat dependent on the space velocity, and increases with increasing space velocity (Fig. 3). The effect of flow rate persists in the presence of added water to a higher flow rate than for the dry standard mixture. The yield of HCN is up to 25%, based on NO converted. Considerably higher yields are likely to be obtainable by suitable choice of the partial pressures of CO, NO and H₂ (4).

Palladium

The yield of HCN in the standard mixture is lower than for Pt by about a factor four at 550–700°C. However, the yield for Pd continues to climb beyond 700°C and overtakes that from Pt at 780°C (Fig. 1). The production of HCN is substantially lowered by the addition of 3.5% H₂O. The inhibiting effect of H₂O is very nearly the same for Pt and Pd.

Ruthenium

The yield of HCN shows a rather different pattern over ruthenium (Fig. 1), in that the maximum yield is reached at low temperature, 500°C, only slightly above the temperature at which HCN becomes first noticeable. The maximum is moreover rather low, 10–15 ppm. However, incorporation of Ru in an ionic form in an oxidic catalyst increases the yield of HCN substantially (see below).

Monel

The production of HCN over monel starts at a much lower temperature than for the noble metal catalysts, viz, below 400°C (Fig. 4). The yield reaches a maximum at 520°C and drops steeply at higher temperatures. The inhibiting effect of H₂O is similar to that for the noble metal catalysts.

Perovskite Catalysts

On $\text{La}_{0.8}\text{K}_{0.2}\text{MnO}_3$ the yield of HCN is very small and its production starts only at temperatures above 600°C (Fig. 5). The maximum level reached in the standard mixture is about the same as for Ru metal, i.e., 10–15 ppm. However, when Ru is incorporated in the oxide as the Ru^{4+} ion, as in $\text{La}_{0.8}\text{K}_{0.2}\text{Mn}_{0.94}\text{Ru}_{0.06}\text{O}_3$, the yield of HCN is increased substantially above that reached on either the matrix perovskite or the metallic Ru. The dependence of the yield of HCN on the temperature of the catalyst remains approximately the same as for Ru metal, with a maximum at about 500°C .

For the $\text{La}_{0.8}\text{K}_{0.2}\text{MnO}_3$ and $\text{La}_{0.8}\text{K}_{0.2}\text{Mn}_{0.94}\text{Ru}_{0.06}\text{O}_3$ catalysts, thermal desorption spectra were obtained. To this end, the catalysts were first equilibrated for 1 hr at 620°C in the catalytic reduction of NO in a mixture of 0.13% NO, 1.3% CO and 0.4% H_2 in He. Subsequently, the temperature was decreased to 150°C , after which the catalyst was soaked in 1% NO in He for 1 hr and cooled to room temperature. Still in 1% NO in He, the sample was

transferred to a silica tube attached to the desorbed gas analysis train with the mass spectrometer. After evacuation to 10^{-4} Torr, the desorption spectra were obtained at a heating rate of $2^\circ\text{C}/\text{min}$. In Fig. 6, the desorption spectrum is shown for $\text{La}_{0.8}\text{K}_{0.2}\text{MnO}_3$. The previously published (9) spectrum for $\text{La}_{0.8}\text{K}_{0.2}\text{Mn}_{0.94}\text{Ru}_{0.06}\text{O}_3$ showed very similar CO and N_2 peaks at $500\text{--}600^\circ\text{C}$, with the ratio of $\text{N}/\text{CO} = 1$. The spectra are different as far as the NH_3 and the HCN peaks are regarded. The HCN peaks found for $\text{La}_{0.8}\text{K}_{0.2}\text{MnO}_3$ are absent in $\text{La}_{0.8}\text{K}_{0.2}\text{Mn}_{0.94}\text{Ru}_{0.06}\text{O}_3$ and the NH_3 evolution in the latter catalyst is completed below 400°C . The difference in the NH_3 evolution has a parallel in the difference of the production of NH_3 over these catalysts in steady-state reduction of NO with CO and H_2 (8, 9). However, the difference in the HCN evolution does not simply parallel the difference in HCN yield for the steady-state flow experiments in Fig. 5. This may conceivably result from the arbitrary choice of 620°C as the equilibration temperature in the temperature-programmed desorption experiments.

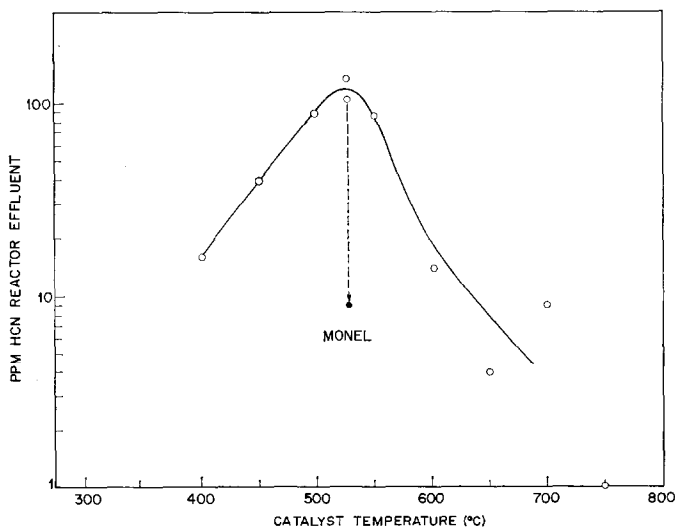


FIG. 4. Yield of HCN vs catalyst temperature for a Cu-Ni (monel) catalyst. (○) standard gas mixture; (●) 3.5% H_2O added. Flow rate: $2.02 \times 10^6 \text{ ml hr}^{-1} \text{ m}^{-2}$.

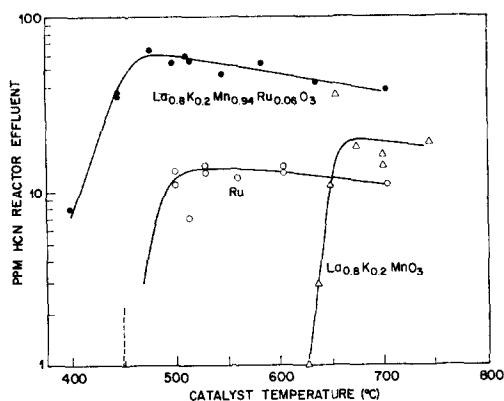


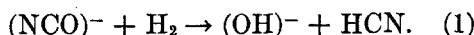
FIG. 5. Yield of HCN vs catalyst temperature for Ru in metallic and oxidic form compared with the yield on the perovskite matrix. Standard gas mixture at the flow rate 3.14×10^6 ml $\text{hr}^{-1} \text{m}^{-2}$ for Ru, 8.43×10^6 ml $\text{hr}^{-1} \text{m}^{-2}$ for $\text{La}_{0.8}\text{K}_{0.2}\text{Mn}_{0.94}\text{Ru}_{0.06}\text{O}_3$, and 8.1×10^6 ml $\text{hr}^{-1} \text{m}^{-2}$ for $\text{La}_{0.8}\text{K}_{0.2}\text{MnO}_3$.

DISCUSSION

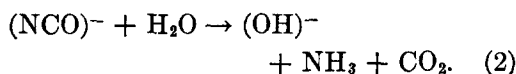
In the reduction of NO by CO and H_2 , the formation of N_2O , N_2 , NH_3 and HCN compete. Since the formation of N_2O is generally limited to the low-temperature regime below 400°C , we need not consider it here. In an atmosphere of NO, CO and H_2 , the intermediate formation of an isocyanate fragment $(\text{NCO})^-$ on the surface is likely for the following reasons. Pt-NCO and $(\text{NCO})^-$ species were identified by isotopic labeling and infrared absorption experiments on the surface of supported Pt catalysts treated with a mixture of NO and CO above 200°C (14). Similarly, Cu-NCO species were found by infrared absorption on copper oxide used in the catalytic reduction of NO (15). NH_4NCO has been produced by the reaction of NH_3 and CO over a heated Pt filament (16) and by the reaction of NO, CO and H_2 over a Pt sponge catalyst (17). The presence of an oxidic support is therefore clearly unnecessary for the formation of the NCO species, contrary to recent suggestions (18). The observation in the present and earlier (8, 9) thermal desorption spectra of simultaneous desorption of N_2

and CO at $500\text{--}600^\circ\text{C}$ in the stoichiometric ratio $\text{N}/\text{CO} = 1$ also supports the presence of an NCO layer at the surface of oxidic catalysts. Thermal decomposition of HNCO similarly yields N_2 and CO (19).

The $(\text{NCO})^-$ surface species is a logical precursor for HCN which may be formed by reduction with either H_2 or CO, e.g.:



The inhibition of the formation of HCN by H_2O may then be due to hydrolysis of the $(\text{NCO})^-$ intermediate:



The lower yield of HCN over Ru, as compared with Pt and Pd is in this mechanism understandable from the lower surface concentration of $(\text{NCO})^-$ on Ru catalysts demonstrated earlier by Unland's ir work (14, 20, 21).

It is interesting that the formation of HCN as a function of temperature runs parallel to the published patterns of NH_3 formation for Cu-Ni (22) and the noble metals (5, 22, 23), except for the low-temperature regime where HCN formation is negligible. However, present data were not gathered to study the mechanism of HCN formation and no definite conclusions regarding the mechanism are warranted.

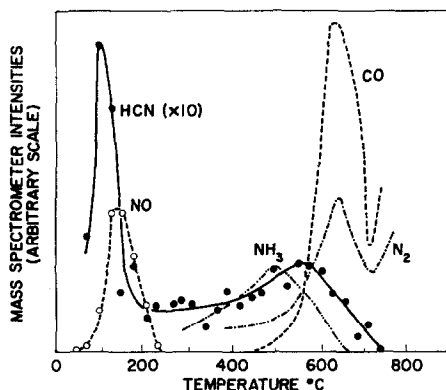


FIG. 6. Desorbed gas analysis for $\text{La}_{0.8}\text{K}_{0.2}\text{MnO}_3$ after use in the reduction of NO with CO and H_2 . Procedure: see text.

Clearly, the formation of HCN requires the hydrogenation of the carbon atom and hence the presence of some hydrogenation function in the catalyst. The ranking of the metal catalysts in terms of HCN formation ($\text{Pt} > \text{Pd} > \text{Cu-Ni} > \text{Ru}$) is in agreement with their ranking as hydrogenation catalysts. In these terms, the effect of the incorporation of Ru in an oxidic matrix is understandable. $\text{La}_{0.8}\text{K}_{0.2}\text{MnO}_3$, when used in the reduction of NO, shows an abundant surface concentration of a species with $\text{N:C:O} = 1:1:1$, as shown by the peaks for CO and N_2 simultaneously desorbing at 600°C (Fig. 6). The hydrogenation activity of manganate perovskites is low however (24) and so is the yield of HCN. Only with the introduction of a hydrogenation function in the form of Ru does the HCN formation increase substantially. The presence of an abundant supply of the NCO surface species increases the HCN formation beyond that over metallic Ru, on which surface the surface concentration of NCO is low. A similar synergistic effect may be the explanation for the higher HCN yield on supported Pt as compared with Pt sponge. Indeed, recent ir work has shown that the NCO-species reside primarily on the oxidic support (18).

CONCLUSIONS

In the reduction of NO with CO and H_2 , hydrogen cyanide is formed at moderately high temperatures. Of the catalysts studied, platinum is the most active in the formation of HCN, with up to 25% conversion of NO into HCN under the conditions employed. The yield of HCN over the catalysts studied decreases in the order $\text{Pt} > \text{Pd} > \text{Cu-Ni} \approx \text{La}_{0.8}\text{K}_{0.2}\text{Mn}_{0.94}\text{Ru}_{0.06}\text{O}_3 > \text{Ru} > \text{La}_{0.8}\text{K}_{0.2}\text{MnO}_3$.

The results suggest that a surface intermediate with the atomic ratio $\text{N:C:O} = 1:1:1$, which may be the isocyanate species discovered by Unland (21), plays

a role in the formation of HCN. For the formation of HCN, hydrogenation of this complex is suggested to compete with hydrolysis to NH_3 .

The synergistic effect observed for Ru and $\text{La}_{0.8}\text{K}_{0.2}\text{MnO}_3$ is suggested to be due to the combination of a high surface concentration of NCO contributed by the oxide surface and the hydrogenation activity contributed by the Ru component.

ACKNOWLEDGMENTS

We thank J. P. Remeika for discussions and for the preparation of the perovskite catalysts in the course of an earlier investigation. We are grateful to E. Vogel and F. Schrey for determinations of surface areas by N_2 and H_2 adsorption.

REFERENCES

1. Sourirajan, S., and Blumenthal, J. L., *Int. J. Air Water Poll.* **5**, 24 (1961).
2. Shelef, M., and Gandhi, H. S., *Ind. Eng. Chem. Prod. Res. Develop.* **11**, 2 (1972).
3. Ullmanns "Encyklopädie der technischen Chemie," 3d ed., Vol. 5, p. 635. Urban and Schwarzenberg, München, 1954.
4. Voorhoeve, R. J. H., Patel, C. K. N., Trimble, L. E., and Kerl, R. J., *Science* **190**, 149 (1975).
5. Dunlevey, F. M., and Lee, C. H., *Science* **192**, 809 (1976).
6. Bradow, R. L., unpublished data.
7. Voorhoeve, R. J. H., and Trimble, L. E., *J. Catal.* **38**, 80 (1975).
8. Voorhoeve, R. J. H., Remeika, J. P., Trimble, L. E., Cooper, A. S., DiSalvo, F. J., and Gallagher, P. K., *J. Solid State Chem.* **14**, 395 (1975).
9. Voorhoeve, R. J. H., Remeika, J. P., and Trimble, L. E., in "The Catalytic Chemistry of Nitrogen Oxides" (R. L. Klimisch and J. G. Larson, Eds.), p. 215-233. Plenum, New York, 1975.
10. Voorhoeve, R. J. H., Remeika, J. P., and Trimble, L. E., *Mater. Res. Bull.* **9**, 1393 (1974).
11. Kreuzer, L. B., and Patel, C. K. N., *Science* **173**, 45 (1971).
12. Patel, C. K. N., Burkhardt, E. G., and Lambert, C. A., *Science* **184**, 1173 (1974).
13. Kreuzer, L. B., Kenyon, N. D., and Patel, C. K. N., *Science* **177**, 347 (1972).
14. Unland, M. L., *J. Phys. Chem.* **77**, 1952 (1973).
15. London, J. W., and Bell, A. T., *J. Catal.* **31**, 96 (1973).

16. Jackson, H., and Northall-Laurie, D., *J. Chem. Soc.* **87**, 433 (1905).
17. Voorhoeve, R. J. H., and Trimble, L. E., unpublished data.
18. Dalla Betta, R. A., and Shelef, M., *J. Molec. Catal.*, in press.
19. Back, R. A., and Childs, J., *Canad. J. Chem.* **46**, 1023 (1968).
20. Unland, M. L., *J. Catal.* **31**, 459 (1973).
21. Unland, M. L., *Science* **179**, 567 (1973).
22. Klimisch, R. L., and Taylor, K. C., *Environ. Sci. Technol.* **7**, 127 (1973).
23. Shelef, M., and Gandhi, H. S., *Ind. Eng. Chem. Prod. Res. Develop.* **11**, 393 (1972).
24. Voorhoeve, R. J. H., and Remeika, J. P., unpublished data.